EURASIAN JOURNAL OF MATHEMATICAL AND COMPUTER APPLICATIONS
ISSN 2306–6172
Volume 12, Issue 4 (2024) 92 – 104

SIMULATION OF SINGLE-PHASE AND TWO-PHASE FLOW THROUGH A SUBMERGED PERFORATED SHEET USING OPENFOAM CODE

Nikulin A.S., Melikhov V.I., Melikhov O.I.

Abstract The aim of the study is to numerically simulate the flow of steam/steam-water mixture through one periodic cell of a submerged perforated sheet, which is an important element of the separation scheme of a horizontal steam generator. The OpenFOAM code is used as a calculation tool. First, the flow of single-phase steam was considered. A comparison of the values of pressure drops on the perforated sheet obtained using the OpenFOAM code for two turbulence models with pressure drops determined by other CFD code FlowVision, various approximate formulas and experimental data shows that the variation of all values does not exceed 10%. The influence of a liquid film on the flow of steam through the hole and the resulting pressure drop is investigated. It is shown that the water film reduces the pressure drop on the perforated sheet by about 6% compared with the flow of single-phase steam.

Key words: hydraulic resistance, submerged perforated sheet, two-phase flow, steam generator, mathematical modeling.

AMS Mathematics Subject Classification: 76T10, 76F65, 76F60.

DOI: 10.32523/2306-6172-2024-12-4-92-104

1 Introduction

In Russian reactor plants with water-water power reactors (VVER), horizontal steam generators (SG) are used to produce saturated steam, which serves as a working medium for a turbine [1, 2]. The vessel of a horizontal SG is a cylindrical vessel with two elliptical bottoms, located horizontally. In the central part of the SG there are two vertical collectors: the inlet, which receives hot water from the reactor core, and the outlet, designed to withdraw the water cooled in the SG into the first circuit of the reactor. The collectors are connected by a large number of U-shaped heat exchange pipes assembled in packages and arranged horizontally, along which the water of the first circuit moves, gradually giving its heat to the water of the second circuit surrounding these pipes. As a result of boiling the water of the second circuit, steam is formed, which enters the turbine. The main requirement for the quality of the generated steam is to maintain the humidity of the steam within the specified limits, since a significant amount of moisture can lead to rapid erosion wear of the turbine blades and its failure.

The separation design used in horizontal SGs is based on gravitational (precipitation) separation, according to which, with relatively small steam loads on the evapora-

tion mirror and a sufficiently high height of the steam volume, a significant number of water droplets due to the action of gravity manage to return to the water volume. Due to the uneven heat release in the volume of horizontal SG, local areas with increased steam load appear on the evaporation mirror near the inlet (hot) collector, which leads to a deterioration of the separation process. To equalize the steam load, a submerged perforated sheet (SPS) is used, which is installed at the steam outlet from the heat exchange tube bundles. The SPS is a device with high hydraulic resistance, which promotes the formation of horizontal steam flows under a perforated sheet from areas with a large steam load to areas with a low steam load, and thereby equalizes the steam load on the evaporation mirror, which is located above the SPS.

Thus, an important parameter of the SPS, which is necessary to calculate the optimal degree of perforation (flow section) of a perforated sheet, is the coefficient of hydraulic resistance of the SPS. Currently, several techniques have been developed to determine the hydraulic resistance coefficient of a perforated sheet [3]-[5], and experimental studies of the hydraulic resistance of SPS have also been conducted [6, 7].

Due to the fact that horizontal SGs for a high-power reactor plant VVER-1500 are characterized by a significantly greater unevenness of the steam load on the evaporation mirror, it was proposed to use SPS with a variable degree of perforation, namely, on the hot side (near the inlet collector) to install sheets with a lower degree of perforation having increased hydraulic resistance, and on the cold side on the side (near the outlet collector) – sheets with a higher degree of perforation (lower hydraulic resistance) [8, 9]. Experiments were performed on the SG stand, which is a model of the upper part of a horizontal SG, to study the alignment ability of SPS with uniform and variable degrees of perforation [10]. In particular, new experimental data were obtained on the values of the hydraulic resistance of SPS, the analysis of which showed that the presence of moisture in the steam stream under certain conditions leads to a decrease in the coefficient of hydraulic resistance [11]. As the reason for this decrease, the hypothesis was put forward that water droplets smooth out the sharp entrance edges of the SPS holes, analysis of model problems using CFD code [12] confirmed the credibility of this assumption.

This article presents the results of numerical simulation of the flow of a steam-water flow through one periodic SPS cell with the OpenFOAM code [13], conducted in order to study the effect of a water film on the hydraulic resistance of SPS.

2 Problem statement, mathematical model and solution method

The geometry of the computational area is shown in Fig. 1. One SPS cell is considered, one side adjacent to the wall, the dimensions shown correspond to the degree of perforation of SPS 5.7%. Steam with a given volume flow rate, which corresponds to a velocity of 0.273 m/s, is supplied at the lower boundary, the upper boundary is open, at which a constant pressure is set, Fig. 2. The ingress of water into the SPS hole is modeled simplistically, the process of movement of water droplets along with the steam flow flowing through the lower boundary, their further precipitation on the lower surface of the sheet and flow through the hole is not considered. Instead, it is assumed that water with a constant flow rate is released on the lower surface of the

sheet (Fig. 2), which then moves under the influence of the steam flow to the hole. This approach allows you to significantly reduce the calculation time and preserve the physics of the process under consideration. It is assumed that water and steam are on the saturation line at a pressure of 7 MPa, thus heat transfer processes are not considered. At the same time, the densities of water and steam have values of 739.7 kg /m^3 and 36.5 kg /m^3, respectively. The specified geometric and thermophysical parameters correspond to the experimental conditions at the SG stand [10, 11].

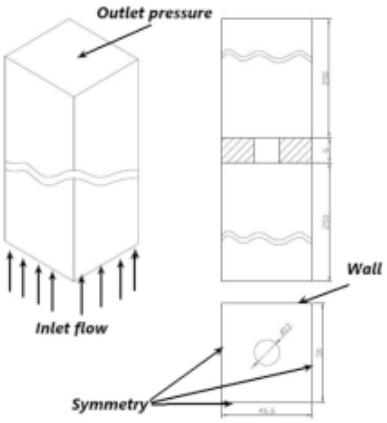

Figure 1: A diagram of the steam flow through the SPS cell, provided that a water film is created on the lower surface of the SPS.

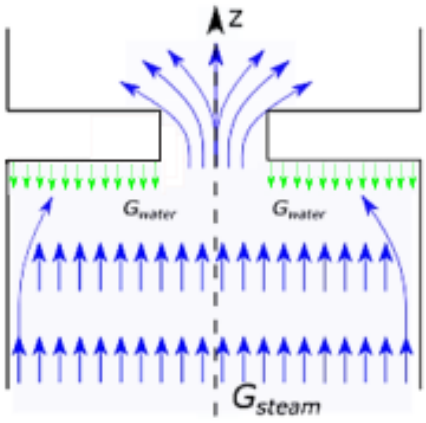

Figure 2: A diagram of the flow of water and steam through the SPS hole.

The CFD code of the OpenFOAM class is used for modeling. The OpenFOAM code is designed to simulate three-dimensional fluid and gas flows in technical and natural objects. The ParaView program is used to visualize these flows using computer graphics methods. The simulated flows include stationary and non-stationary, compressible, slightly compressible and incompressible flows of liquid and gas. The use of various turbulence models and an adaptive computational grid makes it possible to simulate

complex fluid movements, including flows with strong vortex, combustion, and flows with a free surface.

Since the velocities of water and steam in the problem under consideration are small compared to the characteristic velocities of sound in this system and thermal effects are also not taken into account, the compressibility of media can be neglected and considered as incompressible. The hydrodynamic interaction of water and steam occurs at a mobile interphase boundary, which can take on a very complex shape. To simulate such flows, the VOF (Volume-Of-Fluid) method is used [14], the essence of which consists in replacing two immiscible liquids with different properties with one effective liquid with variable properties depending on the volume fractions of the phases. The changes in the volume fractions of the phases are found from the solution of the corresponding transfer equations. The system of defining equations is formulated as follows. The volume fraction of water is denoted by f, then in the calculation cell filled with water, $f= 1$, in the cell filled with steam, $f= 0$, if the interface between steam and water passes in the cell, then $0<f<1$. The transfer equation of the volume fraction of water has the following form:

$$\frac{\partial f}{\partial t} + u_j \frac{\partial f}{\partial x_j} = 0$$

Here t is time, x_j is the j-th dimensional coordinate, u_j is the j-th component of velocity.

The properties of the effective liquid (density ρ and dynamic viscosity μ) in the VOF method are defined as:

$$\rho = (1 - f)\rho_g + f\rho_l, \qquad \mu = (1 - f)\mu_g + f\mu_l.$$

Here the index g is gas (steam), l is liquid (water). For an effective liquid (two-phase medium), the equations of continuity and momentum are solved:

$$\frac{\partial u_j}{\partial x_j} = 0, \qquad \frac{\partial u_i}{\partial t} + \frac{\partial (u_i u_j)}{\partial x_i} = -\frac{\partial P}{\partial x_i} + \frac{\partial}{\partial x_j}\left[\nu_{eff}(\frac{\partial u_i}{\partial x_j} + \frac{\partial u_j}{\partial x_i})\right] + g_i + F_\sigma.$$

Here $\nu_{eff} = \nu + \nu_t$ is the effective kinematic viscosity (the sum of laminar and turbulent viscosities), P is the pressure divided by density, g_i is the acceleration of gravity in the i-th direction, F_σ is the surface tension force at the interface.

Two turbulence models were used in OpenFOAM to calculate the turbulent viscosity:

- kEpsilon (k-ε) is the standard turbulence model [15]. Its application is possible only in high-Reynolds calculations (on a relatively rough grid with wall functions). Here are the fundamental equations for the k-ε turbulence model (1)-(5):

$$\frac{D}{Dt}(\rho k) = \nabla(\rho D_k \nabla k) + \tilde{P}_k - \rho\varepsilon, \tag{1}$$

  where k is a turbulent kinetic energy $[m^2 s^{-2}]$, D_k is a effective diffusivity for k $[m^2/s]$, $\tilde{P}_k$ is a turbulent kinetic energy production rate $[m^2 s^{-3}]$, ε is a turbulent kinetic energy dissipation rate $[kg/ms^3]$,

$$\frac{D}{Dt}(\rho\varepsilon) = \nabla(\rho D_\varepsilon \nabla\varepsilon) + \frac{C_1\varepsilon}{k}\left(\tilde{P}_k + C_3\frac{2}{3}k\nabla u\right) - C_2\rho\frac{\varepsilon^2}{k}, \tag{2}$$

where D_ε is a effective diffusivity for ε $[m^2/s]$,C_1 is a model coefficient, C_2 is a model coefficient,

$$\upsilon_t = C_\mu \frac{k^2}{\varepsilon}, \tag{3}$$

where C_μ is a model coefficient for the turbulent viscosity, υ_t is a turbulent viscosity $[m^2 s^{-1}]$,

$$k = \frac{3}{2}\left(I\left|u_{ref}\right|\right)^2, \tag{4}$$

where I is a turbulence intensity [%] u_{ref} is a reference flow speed $[ms^{-1}]$,

$$\varepsilon = \frac{C_\mu^{0.75} k^{1.5}}{L}, \tag{5}$$

where $C_\mu = 0.09$ is a model constant by default, L is a reference length scale [m],

- kOmegaSST combines both the k-ε model and the k-ω model, which is designed for wall-area resolution approaches [16]. In this model, a new parameter, ω, appears - the specific dissipation of vortices. The equations of the k-ω model are solved in the wall region for this model, and the equations of the k–ε model are solved in the area far from the wall.

Here we present the main equations for the turbulence model SST (6)-(10):

$$\frac{D}{Dt}(\rho\omega) = \nabla(\rho D_\omega \nabla\omega) + \frac{\rho\gamma G}{\nu} - \frac{2}{3}\rho\gamma\omega(\nabla u) - \rho\beta\omega^2 - \rho(F_1 - 1)CD_k\omega + S_\omega \tag{6}$$

$$\frac{D}{Dt}(\rho k) = \nabla(\rho D_k \nabla k) + \rho G - \frac{2}{3}\rho k(\nabla u) - \rho\beta^*\omega k + S_k \tag{7}$$

$$\upsilon_t = a_1 \frac{k}{max(a_1\omega, b_1 F_{23} S)} \tag{8}$$

$$k = \frac{3}{2}\left(I\left|u_{ref}\right|\right)^2 \tag{9}$$

$$\omega = \frac{k^{0.5}}{C_\mu^{0.25} L} \tag{10}$$

The initial conditions for the task: u_g=0.273 m/s, f=0, P=7 MPa. The boundary conditions for the task: for the wall it is u_g=u_l=0, for the lower wall of SPS it is u_l=$V_{l,in}$ m/s ($V_{l,in}$ is a constant velocity), for the inlet it is u_g=0.273 m/s, for the outlet it is P=7 MPa.

The main calculation module for two-phase problems in the OpenFOAM code is interFoam, which allows for hydrodynamic analysis by the VOF method for two incompressible liquids without taking into account phase transitions. The combined solution of the continuity equation and the unsteady momentum equation for an effective liquid is carried out by the PISO method [17], based on a predictor–corrector type scheme. In this method, a preliminary velocity field is located at the predictor stage, which is then refined along with the pressure field during several corrections.

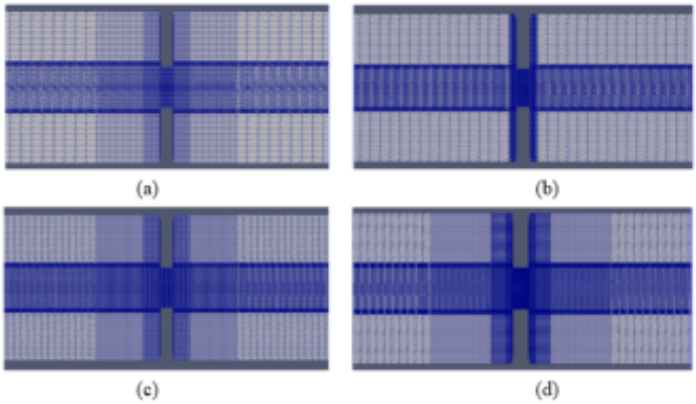

Figure 3: Grid models in longitudinal section: (a) grid No. 1, (b) grid No. 2, (c) grid No. 3, (d) grid No. 4.

3 Equations and mathematics investigation of the influence of the calculated grid and turbulence models

Creating a calculated grid is one of the key aspects in obtaining an accurate simulation result. At the first stage, it is necessary to build a three-dimensional geometric model of the computational domain using a solid-state modeling package. In this work, the Salome [18] package was used, then a structured grid was built in the same package. This grid was then imported into OpenFOAM. Several calculation grids were built, Figs. 3 and 4.

- Grid number 1. The total number of calculated cells was 400 000. The grid has two cell reduction zones before and after the SPS cell. In the central part of the calculation area, cells of a minimum size of $0.08 \times 0.180 \times 0.1$ mm are located near the SPS hole (the cell sizes are specified for the following axes X, Y, Z).

- Grid No.2. The total number of calculated cells was 800 000. The grid has one cell reduction zone before and after the SPS cell. In the central part of the calculation area, cells of a minimum size of $0.075 \times 0.173 \times 0.07$ mm are located near the SPS hole (the cell sizes are specified for the following axes X, Y, Z).

- Grid No. 3 The total number of calculated cells was 1 000 000. The grid has two cell reduction zones before and after the SPS cell. In the central part of the calculation area, cells of a minimum size of $0.07 \times 0.162 \times 0.038$ mm are located near the SPS hole (the cell sizes are specified for the following axes X, Y, Z).

- Grid No. 4. The total number of calculated cells was 1 500 000. The grid has three cell reduction zones before and after the SPS cell. In the central part of the calculation area, cells of a minimum size of $0.06 \times 0.144 \times 0.036$ mm are located near the SPS hole (the cell sizes are specified for the following axes X, Y, Z).

Calculations were performed on each calculation grid using two turbulence models kEpsilon and kOmegaSST. An important parameter characterizing the grid partition

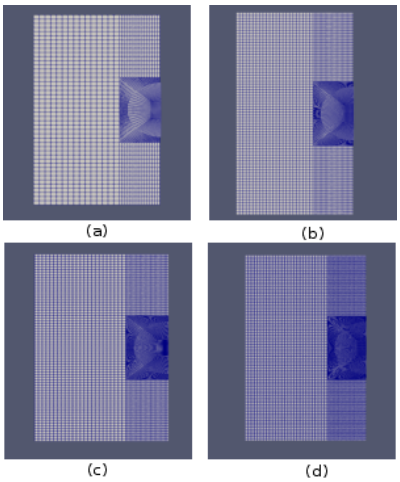

Figure 4: Grid models in cross section: (a) grid No. 1, (b) grid No. 2, (c) grid No. 3, (d) grid No. 4.

in the wall region for turbulent flows is $Y^+ = \sqrt{\tau_w \rho}\, y/\mu$, where τ_w is the friction stress on the wall, y is the normal distance from the wall to the nearest calculation node.The maximum/minimum values of Y^+ on the inner surface of the hole are shown in Tab. 1. To simulate the influence of the wall on turbulence in this problem, scalable (independent of Y^+) wall functions are used, valid in the range $1<Y^+<300$. Thus, it can be concluded that for all grids there is an adequate resolution of the wall area.

The results of calculations of the pressure drop at the SPS and the maximum steam velocity in the hole are shown in Fig. 5. The difference between the parameters obtained on grids No. 3 and No. 4 does not exceed 1%.

Figs. 6 and 7 show the results of pressure and velocity changes along the entire length of the channel along the axis of symmetry, as well as the results of calculations of this task using another CFD code FlowVision [19]. As can be seen from the pressure change graph, the choice of the turbulence model significantly affects the result of the pressure drop. It is worth noting that the results obtained using the k-eps turbulence model are quite lumpy, and when using the SST turbulence model, there is some variation in the values of the pressure drop and maximum velocity. Nevertheless, it can be concluded that the results of the OpenFOAM code are in good agreement with the FlowVision data. Tab. 2 shows the values of the pressure drop on the SPS cell and the values of the maximum velocity in the hole for both calculation codes.

The calculation methods proposed in [3, 5] give relatively close pressure drop values in the range of 932-979 Pa (Tab. 3, 2nd column). However, extrapolation of experimental data on the coefficient of hydraulic resistance SPS for single–phase steam [6, 7] to the parameters of the problem considered in this article leads to a lower value 837 Pa. Note that in [3] it is reported that the experimental data in all cases are below the values obtained by this method, while the difference is within 2-15% and in exceptional cases can reach 22%. It can be assumed that a similar discrepancy also occurs for methods very close to [3, 4, 5]. Then, assuming that the real pressure drops on the SPS deviate from the values calculated according to these methods by 15%, we obtain a range of pressure drop values of 810-851 Pa (Tab. 3, 3rd column), which is in good agreement with the value of 837 Pa based on experimental data [6, 7].

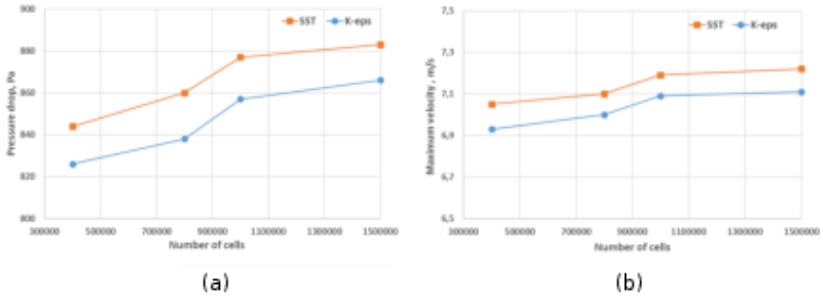

Figure 5: Influence of the grid on (a) the pressure drop for different turbulence models,(b) the maximum velocity for different turbulence models.

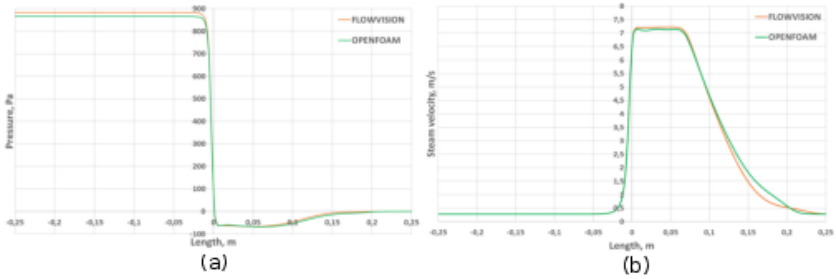

Figure 6: Graph of pressure (a) and velocity b) changes along the length of the channel, using the k-epsilon turbulence model.

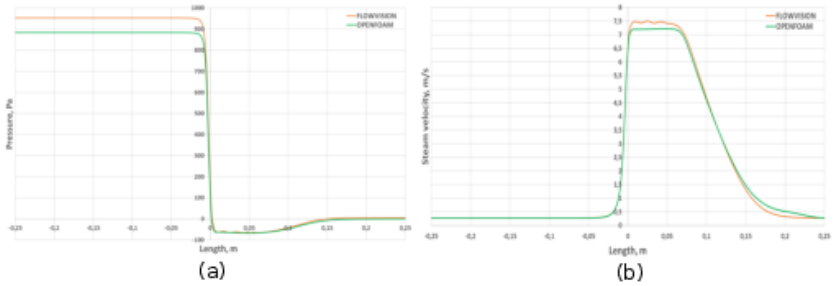

Figure 7: Graph of pressure (a) and velocity (b) changes along the length of the channel, using the SST turbulence model.

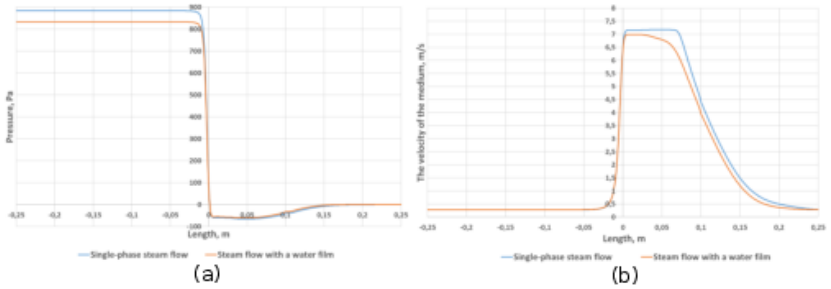

Figure 8: Graph of pressure drop (a) and velocity (b) along the length of the channel.

Thus, the following conclusions can be drawn:

1. All the results of calculations of the pressure drop on the SPS using the FlowVision and OpenFOAM codes for two turbulence models are close to each other, the error does not exceed 10%;

2. A comparison of the values of pressure drops on the SPS obtained using the FlowVision and OpenFOAM codes for two turbulence models with pressure drops determined by various calculation methods and experimental data shows that the value spread also does not exceed 10%.

For further analysis of the effect of the liquid film on the hydrodynamics of steam flow through the SPS hole, the SST turbulence model was selected.

4 The influence of the water film on the hydraulic resistance of SPS

For the problem of saturated steam flowing through one SPS cell in the existence of a water film, a modified calculation grid No. 4 was used. For better resolution of a thin film of liquid moving along the lower surface of the perforated sheet, several layers of calculation cells were added in the area adjacent to this surface. As a result, the total number of settlement cells in this case amounted to 2.5 million. Calculations of the single-phase steam flow on grid No. 4 and modified grid No. 4 give the same results.

As mentioned above, the process of formation of a liquid film on the lower surface of the SPS as a result of the removal of water droplets by a steam stream from pipe

Table 1: Maximum/minimum values of Y^+ on the inner surface of the hole

Model	Grid №1	Grid №2	Grid №3	Grid №4
kEpsilon	127/21	97/14	56/11	31/5
kOmegaSST	128/26	106/20	68/15	37/7

Table 2: Values of the pressure drop on the SPS and the maximum velocity in the hole

	Pressure drop Δ P, Pa	Maximum velocity value V_{max}, m/s
The k-ε turbulence model		
FlowVision	884	7.22
OpenFOAM	866	7.11
The SST turbulence model		
FlowVision	954	7.50
OpenFOAM	883	7.22

Table 3: The values of the pressure drop on the SPS calculated by various methods

Method	Pressure drop ΔP, Pa (according to the method)	Pressure drop ΔP, Pa (according to the method - 15%)
Idelchik (1960) [3]	932	810
RD-91 [4]	939	817
Idelchik (2007) [5]	979	851

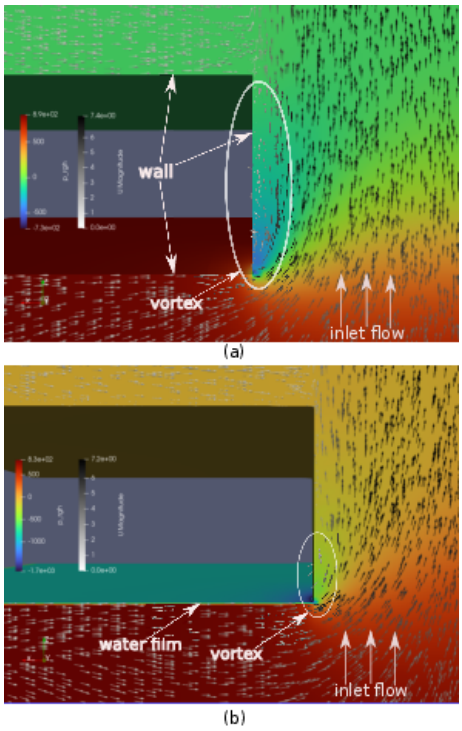

Figure 9: Vector field and pressure field (a) without a water film, (b) with a water film

bundles and their precipitation on this surface was not considered in the problem. It was assumed that on the lower surface of the sheet, water is supplied at a given flow rate and then, under the influence of steam flowing from the lower boundary, it is carried up through the hole. The water flow rate was selected in such a way that during the typical time of the process under study, when a pressure drop was established on the diaphragm, a thin layer of liquid formed on the lower surface of the diaphragm. For the calculation given below, this flow rate was 0.0648 g/s, which corresponds to the humidity of the two-phase flow, which is the ratio of water flow to total flow, 0.28%.

Fig. 8 shows comparative graphs of the pressure drop and velocity changes along the length of the channel during the flow of single-phase steam and in the presence of a water film on the lower surface of the SPS. The water film reduces the pressure drop on the SPS by smoothing the sharp edges at the entrance to the hole, as a result of which the steam flow through the hole becomes smoother. The pressure drop at the SPS hole during the flow of single–phase steam was 883 Pa, and the pressure drop for the flow of steam in the presence of a water film was 832 Pa. Thus, the presence of a water film reduces the pressure drop by about 6%.

As can be seen from Fig. 9, in the presence of a water film, the vortices in the hole of the SPS cell become smaller, but it should be noted that they do not disappear completely. Fig. 10 shows the current lines in the SPS hole without a water film and, if there is one, as can be seen, in the absence of a water film, the vortices are more intense, which leads to a higher pressure drop.

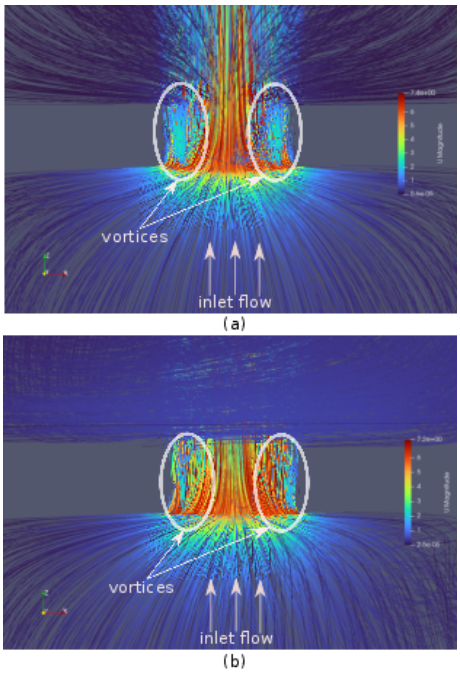

Figure 10: Flow lines (a) without a water film, (b) with a water film

5 Conclusion

The article presents a numerical simulation of the flow of steam and steam-water mixture through one periodic SPS cell using the OpenFOAM code. The calculated area is a parallelepiped, at the lower input boundary of which a constant steam velocity is set, at the upper boundary – the conditions for free exit of the medium, at the lateral boundaries – either symmetry conditions or a solid wall. In the middle part of the calculation area, a sheet of a given thickness with one hole is installed. The OpenFOAM computational fluid dynamics code is used as the main calculation tool. First, the flow of single-phase steam was considered. The mathematical model included Reynolds-averaged equations of incompressible fluid motion supplemented by a semi-empirical turbulence model. A study of the grid convergence of the solution on four successively thickening grids was performed. The influence of two different turbulence models on the solution is considered. Cross-verification with the FlowVision code has been performed.

It was found that all the results of calculations of the pressure drop on the SPS using the FlowVision and OpenFOAM codes for two turbulence models are close to each other, the error does not exceed 10%. A comparison of the values of pressure drops on the SPS obtained using the FlowVision and OpenFOAM codes for two turbulence models with pressure drops determined by various calculation methods and experimental data shows that the difference in values also does not exceed 10%.

The Influence of the liquid film on the flow of steam through the hole and the resulting pressure drop was investigated. It was assumed that on the lower surface of the sheet, water is supplied at a given flow rate and then, under the influence of steam flowing from the lower boundary, it is carried up through the hole. To simulate the

evolution of a two-phase medium, the VOF method was used, which allows tracking the movement of the interphase boundary. It is shown that the water film reduces the pressure drop on the SPS by about 6% compared to the flow of single-phase steam by smoothing the sharp edges at the entrance to the hole, due to this, the flow of steam through the hole becomes smoother.

Acknowledgement

The reported study was funded by the Russian Science Foundation (RSF), Project No. 22-19-00793, https://rscf.ru/en/project/22-19-00793/. The calculations were performed on the computing resources of the Joint SuperComputer Center of the Russian Academy of Sciences, https://www.jscc.ru/.

References

[1] Lukasevich B.I., Trunov N.B., Dragunov Y.G., Davidenko S.E., *Steam Generators of WWER Reactors for Nuclear Power Plants*. 2004, (In Russian).

[2] Papp L., Vacek J., *WWER steam generators*. Steam Generators for Nuclear Power Plants, Ed. J. Rizic., 1st Edition, Woodhead Publishing Series in Energy, 2017, 107-124.

[3] Idelchik I.E., *Consideration of the effect of viscosity on the hydraulic resistance of diaphragms and grates*. Therm. Eng., (1960), 75-80 (In Russian).

[4] *Methodological guidelines. Thermal and hydraulic calculation of nuclear power plant heat exchange equipment, RD 24.035.05-89*. Ministry of Heavy, Power engineering and Transport Construction of the USSR, 1991 (In Russian).

[5] Idelchik I.E., *Hydraulic Resistance Handbook*. Begell House, 2007.

[6] Ryabov G.A., Karasev V.B., Kozlov Yu.V., *Experimental study of the hydraulic resistance of perforated sheets on a steam-water mixture*. Therm. Eng., 6. (1984), 68-70 (In Russian).

[7] Ryabov G.A., Kozlov Yu.V., *Experimental study of the hydrodynamics of submerged perforated sheets*. Therm. Eng., 8. (1984), 62-65 (In Russian).

[8] Trunov N.B., Sotskov V.V., Levchenko Yu.D., *Improved PGV-1500 separation system*. Heavy engineering, 1. (2008), 8–13 (In Russian).

[9] Sotskov V.V., *Development and research of an upgraded design of steam generator separation devices for nuclear power plants with high-power VVER reactors*. Ph.D. Thesis. Podolsk: OKB "Gidropress", 2010,(In Russian).

[10] Blinkov V.N., Elkin I.V., Melikhov V.I., Nerovnov A.A., Emelianov D.A., Melikhov O. I., Nikonov S. M., Parfenov Y.V., *Influence of non-uniformity of the submerged perforated sheet on steam demand leveling on the evaporation surface of a vver steam generator*. Therm. Eng., 63. 1. (2016), 51-55.

[11] Blinkov V.N., Elkin I.V., Melikhov V.I., Nerovnov A.A., Emelianov D.A., Melikhov O. I., Nikonov S. M., Parfenov Y.V., *The influence of void fraction on the submerged perforated sheet hydraulic friction factor*. Therm. Eng., 62. 7. (2015), 484-489.

[12] Melikhov V. I., Melikhov O. I., Nerovnov A. A., Nikonov S. M., *Investigation into behavior of a steam-water mixture flow through holes in a submerged perforated sheet at high void fractions.* Therm. Eng., 65. 1. (2018), 45-50.

[13] OpenFOAM, *Computer software.* Date of the last access (2024, May 20). Retrieved from https://www.openfoam.com

[14] Hirt C. W., Nichols B. D., *Volume of Fluid (VOF) method for the dynamics of free boundaries.* Journal of Computational Physics, 39. (1981), 201-225.

[15] Launder B.E., Spalding D.B., *The numerical computation of turbulent flows.* Computer Methods in Applied Mechanics and Engineering, 3.2 (1974), 269–289.

[16] Menter F.R., Kuntz M., Langtry R., *Ten years of industrial experience with the SST turbulence model.* Proceedings of the 4th International Symposium on Turbulence, Heat and Mass Transfer (2003), 625–632.

[17] Issa R.I., *Solution of the implicitly discretised fluid flow equations by operator-splitting.* Journal of Computational Physics, 62. (1986), 40-65.

[18] Salome, *Computer software.* Date of the last access (2024, May 25). Retrieved from https://www.salome-platform.org

[19] Melikhov V.I., Nikulin A.S., *Computational analysis of the steam-water flow through a submerged perforated sheet.* E3S Web of Conferences, 459. (2023), 1-6.

A.S. Nikulin,
National Research University "Moscow Power Engineering Institute",
Krasnokazarmennaya 14, Moscow 111250, Russian Federation,
Email: iskander0215@gmail.com,

V.I. Melikhov,
National Research University "Moscow Power Engineering Institute",
Krasnokazarmennaya 14, Moscow 111250, Russian Federation,
Email: volodymyr.mel@yandex.ru,

O.I. Melikhov,
National Research University "Moscow Power Engineering Institute",
Krasnokazarmennaya 14, Moscow 111250, Russian Federation,
Email: oleg.melikhov311@yandex.ru.

Received 12.08.2024, Accepted 02.10.2024